Available online at www.sciencedirect.com

ScienceDirect

Nuclear Physics B 895 (2015) 272–287

NUCLEAR PHYSICS B

www.elsevier.com/locate/nuclphysb

Skyrmions with low binding energies

Mike Gillard *, Derek Harland, Martin Speight

School of Mathematics, University of Leeds, Leeds LS2 9JT, UK

Received 30 January 2015; received in revised form 1 April 2015; accepted 7 April 2015

Available online 11 April 2015

Editor: Stephan Stieberger

Abstract

Nuclear binding energies are investigated in two variants of the Skyrme model: the first replaces the usual Skyrme term with a term that is sixth order in derivatives, and the second includes a potential that is quartic in the pion fields. Solitons in the first model are shown to deviate significantly from ansätze previously assumed in the literature. The binding energies obtained in both models are lower than those obtained from the standard Skyrme model, and those obtained in the second model are close to the experimental values.
© 2015 The Authors. Published by Elsevier B.V. This is an open access article under the CC BY license (http://creativecommons.org/licenses/by/4.0/). Funded by SCOAP^3.

1. Introduction

The Skyrme model is a candidate model of nuclear physics in which nuclei appear as topological solitons. It can be derived from QCD as an effective theory valid in the limit of an infinite number of colours [1]. It successfully reproduces a number of qualitative features of nuclei, including quantum numbers of excited states [2] and the stability of the alpha-particle [3]. Quantitative features are generally predicted with reasonable accuracy, but with some notable exceptions. One class of quantities which are not accurately predicted within the standard Skyrme model is that of nuclear binding energies: typically, these are too large by an order of magnitude.

In the last few years a number of variants of the Skyrme model have been proposed which aspire to rectify this problem. Among them are a holographic model that incorporates vector

* Corresponding author.
E-mail addresses: m.n.gillard@leeds.ac.uk (M. Gillard), d.g.harland@leeds.ac.uk (D. Harland), speight@maths.leeds.ac.uk (M. Speight).

http://dx.doi.org/10.1016/j.nuclphysb.2015.04.005
0550-3213/© 2015 The Authors. Published by Elsevier B.V. This is an open access article under the CC BY license (http://creativecommons.org/licenses/by/4.0/). Funded by SCOAP^3.

mesons [4], the near BPS sextic model [5], and the lightly bound model [6]. This article contains a thorough investigation of binding energies in the latter two. These models have in common that they supplement Skyrme's Lagrangian with terms involving the pion fields only.

The Skyrme Lagrangian takes the form

$$\mathcal{L} = \frac{F_\pi^2}{16\hbar}\mathrm{Tr}(R_\mu R^\mu) + \frac{\hbar}{32g^2}\mathrm{Tr}([R_\mu, R_\nu], [R^\mu, R^\nu]) + \frac{F_\pi^2 m_\pi^2}{8\hbar^3}\mathrm{Tr}(1-U) + \dots . \tag{1.1}$$

Here $U(x)$ is an $SU(2)$-valued field, $R_\mu = (\partial_\mu U)U^\dagger$ is its right-invariant current, F_π and m_π denote the pion decay constant and mass, and g is a dimensionless parameter. This Lagrangian should be understood as defining an effective field theory, and the ellipsis represents additional terms which are higher order either in derivatives or in the pion fields $1-U$. The baryon number of a field $U(x)$ is defined to be

$$B(U) = -\frac{1}{24\pi^2}\int_{\mathbb{R}^3} \epsilon_{ijk}\mathrm{Tr}(R_i R_j R_k)\mathrm{d}^3x = \frac{1}{2\pi^2}\int_{\mathbb{R}^3} \mathcal{B}\mathrm{d}^3x, \tag{1.2}$$

and is equal to the degree of the restriction of U to any spatial slice.

The sextic model adds to Skyrme's Lagrangian a term sextic in derivatives. The motivation for doing so is that a Skyrme model with only a sextic term and a potential term is BPS: energies are directly proportional to the baryon number, and hence binding energies are zero. Thus a Skyrme model that includes a potential and a sextic term with coefficients much larger than the other terms might reasonably be expected to have low binding energies.

The lightly bound model does not include any terms of higher order in derivatives but instead includes an additional potential term proportional to $\mathrm{Tr}(1-U)^4$. The model whose Lagrangian consists only of this term and the Skyrme term has an exact solution with baryon number 1 but has no solutions of higher baryon number which are stable to fission; nuclei are unbound in this model. One therefore expects the Skyrme model that includes this potential with a large coefficient to have low binding energies. Simulations of a two-dimensional toy model support this hypothesis [7].

In the sequel, numerical approximations to energy minima in both models will be presented for baryon numbers one to eight. These results are consistent with the hypotheses that low binding energies are attainable in both models. However, the sextic model has proved more challenging to simulate numerically and we have not been able to obtain reliable results for soliton energies in the parameter regime in which binding energies are expected to be comparable to those of real nuclei. The structures of energy minima obtained in the sextic model differ radically from those previously assumed in the literature [5,8–11]; thus a re-examination of the results obtained in these papers seems to be warranted. The energy minima obtained in the lightly bound model differ from those in the standard Skyrme model in two respects: their symmetry groups are smaller; and they have the structure of ensembles of particles. The sextic model will be discussed in Section 2 and the lightly bound model in Section 3; some conclusions will be drawn in Section 4.

2. The sextic model

In this section we study a one-parameter family of models with energy

$$E_\varepsilon = \int_{\mathbb{R}^3} \left(-\frac{\varepsilon}{4}\mathrm{Tr}R_i R_i + \frac{1}{2}\left(\frac{1}{12}\epsilon_{ijk}\mathrm{Tr}(R_i R_j R_k)\right)^2 + \frac{1}{8}(\mathrm{Tr}(1-U))^2 \right)\mathrm{d}^3x, \tag{2.1}$$

$\varepsilon \geq 0$ being the parameter. So, we have replaced the usual Skyrme term with a sextic term proportional to $\mathcal{B}^2$, and modified the potential. The regime of interest is when ε is positive and small. The choice of potential is motivated by two facts: skyrmions in the $\varepsilon = 0$ model are *compactons*, which is numerically convenient (strongly localised solitons are less prone to finite box effects), and this potential is *massless*. That is, the expansion of the potential about $U = 1$ has no quadratic terms, so the pions in this theory are massless. This is important because, were the pion mass non-zero, it would scale like ε^{-1}, and hence would be unphysically large in the regime of interest.

It is convenient for our purposes to think of the Skyrme field as taking values in S^3 rather than $SU(2)$. Thus we define $\varphi_0, \ldots, \varphi_3$ so that

$$U = \varphi_0 \mathbb{I}_2 + i\varphi_1\tau_1 + i\varphi_2\tau_2 + i\varphi_3\tau_3 \tag{2.2}$$

where τ_1, τ_2, τ_3 are the Pauli matrices, and $\varphi_0^2 + \varphi_1^2 + \varphi_2^2 + \varphi_3^2 = 1$. In terms of the field $\varphi : \mathbb{R}^3 \to S^3 \subset \mathbb{R}^4$, the energy of interest is

$$E_\varepsilon = \frac{1}{2} \int_{\mathbb{R}^3} \left(\varepsilon |\mathrm{d}\varphi|^2 + |\varphi^* \Omega|^2 + \mathcal{U}(\varphi)^2 \right) \mathrm{d}^3 x, \tag{2.3}$$

where Ω is the usual volume form on the unit 3-sphere and

$$\mathcal{U} : S^3 \to \mathbb{R}, \qquad \mathcal{U}(\varphi) = 1 - \varphi_0. \tag{2.4}$$

This formulation of the model makes manifest the simple, but crucial, fact that E_0 is invariant under volume-preserving diffeomorphisms of $\mathbb{R}^3$ [5]: given any field φ and any diffeomorphism $\psi : \mathbb{R}^3 \to \mathbb{R}^3$ such that

$$\psi^*(\mathrm{d}x_1 \wedge \mathrm{d}x_2 \wedge \mathrm{d}x_3) = \mathrm{d}x_1 \wedge \mathrm{d}x_2 \wedge \mathrm{d}x_3, \tag{2.5}$$

$E_0(\varphi \circ \psi) = E_0(\varphi)$. It will be convenient to introduce the shorthand

$$E_\varepsilon = \varepsilon E^{(2)} + E^{(6)} + E^{(0)}, \tag{2.6}$$

the superscript indicating the degree of the corresponding piece of the energy density as a polynomial in spatial partial derivatives.

As is well known [5,12,13], in the case $\varepsilon = 0$ this model is BPS:

$$E_0 \geq c_{\mathcal{U}} B, \qquad c_{\mathcal{U}} = \int_{S^3} \mathcal{U}, \tag{2.7}$$

with equality if and only if

$$\varphi^* \omega = U(\varphi)\, \mathrm{d}x_1 \wedge \mathrm{d}x_2 \wedge \mathrm{d}x_3, \tag{2.8}$$

or, equivalently, $\mathcal{B} = \mathcal{U}$. For our choice of potential, $c_{\mathcal{U}} = Vol(S^3) = 2\pi^2$ (since $\int_{S^3} \varphi_0 = 0$) and solutions of (2.8) have compact support, meaning $\phi(x) = v = (1, 0, 0, 0)$, the vacuum value, for all x outside some bounded subset of $\mathbb{R}^3$. Eq. (2.8) can be interpreted as the condition that φ is a volume-preserving map from the subset of $\mathbb{R}^3$ on which $\phi \neq v$ to $S^3 \backslash \{v\}$ equipped with the deformed volume form $\Omega'_{\mathcal{U}} = \Omega / \mathcal{U}$. From this we deduce that any $B = 1$ BPS skyrmion (solution of (2.8)) occupies a total volume of

$$Vol_1 = \int_{S^3 \backslash \{v\}} \Omega'_{\mathcal{U}} = 4\pi^2 \tag{2.9}$$

and $Vol_B = B\, Vol_1$, in obvious notation. There is a $B = 1$ solution within the hedgehog ansatz,

$$\varphi_H(r\boldsymbol{n}) = (\cos f(r), \sin f(r)\boldsymbol{n}), \tag{2.10}$$

where the profile function has $f(0) = \pi$, $f(\infty) = 0$, and satisfies the ODE

$$-\frac{df}{dr}\frac{\sin^2 f}{r^2} = 1 - \cos f. \tag{2.11}$$

An implicit solution to this boundary value problem is given by

$$-\tfrac{1}{3}r^3 = f - \pi + \sin f. \tag{2.12}$$

There are many ways to construct charge B BPS skyrmions. One can, for example, superpose B charge 1 solutions (e.g. hedgehogs) with disjoint support. Less trivially, one can precompose a charge 1 solution with a volume-preserving B-fold covering map $\mathbb{R}^3\backslash\mathbb{R} \to \mathbb{R}^3\backslash\mathbb{R}$, for example

$$\psi_B : \mathbb{R}^3\backslash\mathbb{R}_z \to \mathbb{R}^3\backslash\mathbb{R}_z, \qquad \psi_B : (r, \theta, \phi) \mapsto (B^{-1/3}r, \theta, B\phi), \tag{2.13}$$

in spherical polar coordinates. Previous phenomenological studies of BPS [5,8,9] and near-BPS [10,11] skyrmions have all been based on BPS skyrmions of this type. Note that, by their very construction, these BPS skyrmions have spherically symmetric baryon density (they start with a hedgehog, then precompose with a map which preserves $\mathcal{B}$).

To simulate the model with $\varepsilon > 0$ numerically, we put it on a cubic lattice of size N^3 with lattice spacing h, typical values being $N \approx 151\sqrt[3]{B}$ and $h = 0.05$, so that the box length hN is, for each B, roughly twice the radius of the BPS skyrmion given by (2.13). Dirichlet boundary conditions are imposed (so $\varphi = v$ on the boundary of the cube). We replace spatial partial derivatives by 4th order accurate difference operators to obtain a lattice approximant to E_ε. Starting at $\varepsilon = 1$ with some initial choice of φ, this lattice energy is then minimised using a gradient-based minimisation algorithm (the quasi-Newton L-BFGS method, limited memory version). Having found a (perhaps only local) minimum of E_1, we then decrease ε slightly and, using the E_1 minimiser as initial data, minimise again. Iterating this process we construct a curve of local E_ε minimisers, parametrised by ε. To increase our chance of finding the global minimiser of E_ε, we repeat the process with a variety of initial guesses at $\varepsilon = 1$ (generated by, *inter alia*, the rational map ansatz, and the product ansatz applied to sets of lower charge solutions), obtaining conjectured global minimisers for all charges from 1 to 8. Using the same differencing scheme, we also construct a lattice approximant B_{num} to B. For all the results we will report we find that this is accurate (i.e. integer valued) to within 0.01% but is always lower than B. We take this as a rough measure of the expected accuracy of our energies. Finite box simulations generically underestimate energies because they exclude the contribution of the soliton tail. We compensate for this by reporting $E = (B/B_{num})E_\varepsilon$.

As well as monitoring the accuracy of B, we also keep track of the Derrick scaling constraint, as in [14]. That is, any critical point of E_ε should, by the Derrick scaling argument [15], satisfy the virial constraint

$$D(\varepsilon) := \frac{1}{E_\varepsilon}(3E^{(6)}(\varepsilon) - \varepsilon E^{(2)}(\varepsilon) - 3E^{(0)}(\varepsilon)) = 0. \tag{2.14}$$

In a finite box, large enough that boundary pressure is negligible, $D(\varepsilon)$ should be small and positive [14]. If $D(\varepsilon)$ becomes negative, or large and positive, this indicates that our numerical solution is not reliable, and we discard it. In all the simulations reported here, we find that $D(\varepsilon)$ remains small (less than 1.5%) for all $\varepsilon \in [0.2, 1]$ but then explodes shortly below $\varepsilon = 0.2$ when

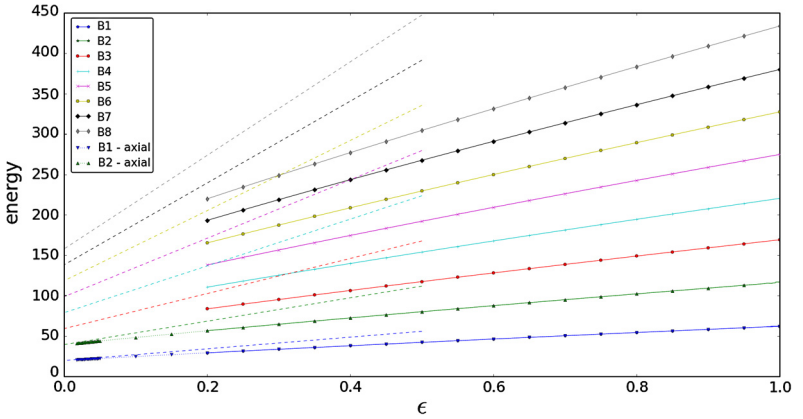

Fig. 1. Minimum energies in the charge B sector for $B = 1, \ldots, 8$, as a function of ε. The dashed lines show the upper bound derived in Eq. (2.15). The dotted lines show the minimum energies for $B = 1, 2$ as a function of ε when restricted to axial symmetry.

$B > 1$. Simultaneously to the bad violation of $D(\varepsilon) = 0$, we find that the numerical solutions develop spike-like singularities, indicating the development of spatial structures smaller than the resolution of our lattice. Once this occurs, we can no longer track the solution curve. We conclude, then, that the model is numerically inaccessible (at least with our methods) for $0 \leq \varepsilon < 0.2$. We will see shortly that, for $B = 1$ and $B = 2$, other methods can be used that allow us to get much closer to $\varepsilon = 0$, but these rely on the enhanced symmetry of these cases.

Let us denote by $E_{min}(B, \varepsilon)$ the energy of the global minimiser of E_ε of charge B (assuming that such exists). It is clear from the definition of E_ε that this is a monotonically increasing function of ε, and that $E_{min}(B, 0) = 2\pi^2 B$. It is bounded above by the total energy of any charge B BPS solution, for example, a superposition of B hedgehogs of disjoint support. Hence

$$E_{min}(B, \varepsilon) \leq B(2\pi^2 + \varepsilon E^{(2)}(\varphi_H)) \approx (19.74 + 72.36\varepsilon)B, \tag{2.15}$$

so $E_{min}(B, \varepsilon)$ converges to $2\pi^2 B$ as $\varepsilon \to 0$. Fig. 1 shows a plot of $E_{min}(B, \varepsilon)$ for $B = 1, \ldots, 8$, $0.2 \leq \varepsilon \leq 1$, as predicted by our numerical data. The energy value for $B = 8$ is taken from the minimum energy configuration at each sampled value of ε. Energy and baryon number data for $\varepsilon = 1, 0.2$ can be found in Appendix A, Table 2.

Fig. 2 presents, for each degree from $B = 1$ to $B = 8$, a pair of energy minimisers, for $\varepsilon = 1$ (left image) and $\varepsilon = 0.2$ (right image). In each case, a surface of constant baryon density is shown, and the colouring of each point represents the orientation of $\boldsymbol{\varphi} = (\varphi_1, \varphi_2, \varphi_3)$ there. Since the $B = 1$ minimisers are within the hedgehog ansatz, their pictures specify the colouring scheme: we radially project $\boldsymbol{\varphi}$ onto the unit cube $\max\{|\varphi_1|, |\varphi_2|, |\varphi_3|\} = 1$ and colour each face of the cube: where $(\pm 1, 0, 0)$ are yellow/cyan, $(0, \pm 1, 0)$ are red/green and $(0, 0, \pm 1)$ are white/black. Except for $B = 6$, the $\varepsilon = 1$ minimisers are qualitatively similar to those of the usual Skyrme model with a pion mass: in both cases, the potential strongly penalises fields where ϕ is close to $-v$ over large regions, and hence, disfavours the hollow shell-like minimisers found in the Skyrme model without a potential, preferring the formation of chain-like structures. (The $B = 6$ skyrmion suggests that this effect becomes important at lower B for our choice of potential than for the standard pion mass potential.) Swapping the quartic Skyrme term for the sextic term does not seem to have made a qualitative difference to the skyrmions. A similar observation was made by Floratos and Piette [16], who found that the energy minimisers (for $B = 1$ to 5) in the

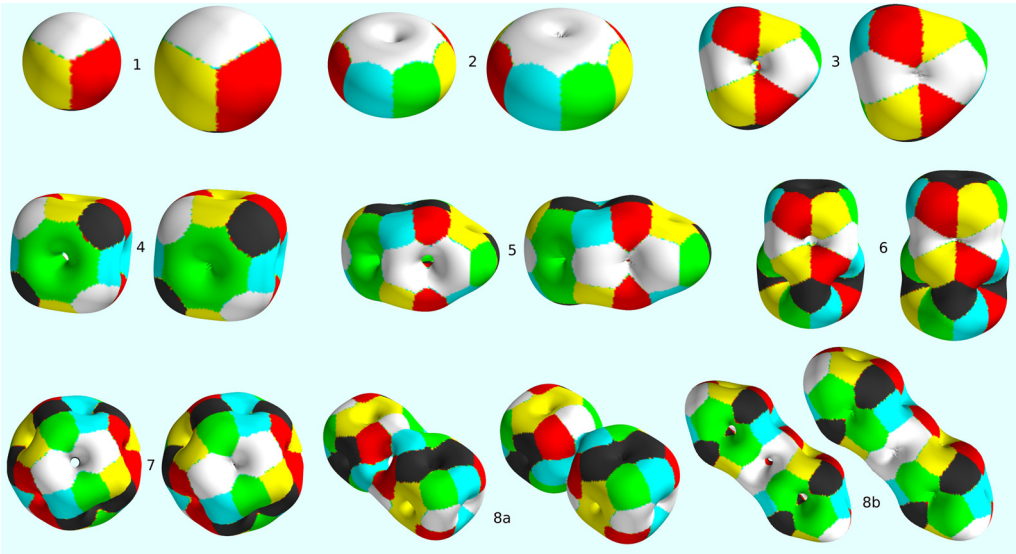

Fig. 2. Level sets of baryon density for skyrmions in the sextic model with $\varepsilon = 1$ (left) and $\varepsilon = 0.2$ (right), degrees $B = 1$ to $B = 8$. On each surface $\mathcal{B} = 0.5 \max\{\mathcal{B}(x)\}$.

sextic model with *no* potential were qualitatively similar to those of the usual *massless* Skyrme model. We present two local minimisers for $B = 8$, labelled $8a$ and $8b$. At $\varepsilon = 1$ it is clear that $8a$ has lower energy (by 0.35%), but at $\varepsilon = 0.2$ the energy difference is close to our numerical accuracy, and $8b$ is slightly lower.

Comparing the $\varepsilon = 0.2$ minimisers with their $\varepsilon = 1$ counterparts, we find that as ε reduces, the skyrmions have a tendency to lose symmetry, the holes in the level sets of $\mathcal{B}$ tend to shrink, and $\mathcal{B}$ tends to become more uniform within the skyrmion core. The density of nuclear matter is roughly constant in real nuclei, so this effect is desirable, since it reproduces at a classical level a feature that may emerge only after quantisation in the conventional Skyrme model. It is along rays emerging through the holes, on which $\mathcal{B} = 0$, that singularities begin to form as ε drops below 0.2. This is consistent with the hypothesis that, as $\varepsilon \to 0$, the minimisers converge to low regularity solutions of the Bogomol'nyi equation (2.8): such a solution must develop singularities wherever $\mathcal{B} = 0$ and $\varphi \neq v$. A more detailed picture of this process can be seen in Fig. 3, which shows plots of $\mathcal{B}$ along a line through the centre of the $B = 4$ skyrmion, again for $\varepsilon = 1$ and $\varepsilon = 0.2$. This line pierces the cube diagonally through a pair of maximally separated corners. Also plotted is the (square root) potential density $\mathcal{U}$ for $\varepsilon = 0.2$, suggesting that φ is converging, as $\varepsilon \to 0$, to a continuous but not differentiable solution of $\mathcal{B} = \mathcal{U}$.

Except for $B = 1$ and $B = 2$, there is no evidence that φ is converging to a BPS skyrmion with axial symmetry. In the case $B = 2$, φ appears to converge to a BPS skyrmion with axial symmetry, but not one for which $\mathcal{B}$ is spherically symmetric. This casts doubt on the validity of phenomenological studies of BPS and near BPS skyrmions based on fields of the form $\varphi_H \circ \psi_B$ (see Eq. (2.13)) [5,8–11]. Such studies perform a rigid body quantisation, and depend strongly on the isospin and spin inertia tensors of the BPS skyrmions used,

$$I_{ij}(\varphi) = \int_{\mathbb{R}^3} \mathrm{d}\varphi_0 \wedge \mathrm{d}\varphi_i \wedge *(\mathrm{d}\varphi_0 \wedge \mathrm{d}\varphi_j) + O(\varepsilon),$$

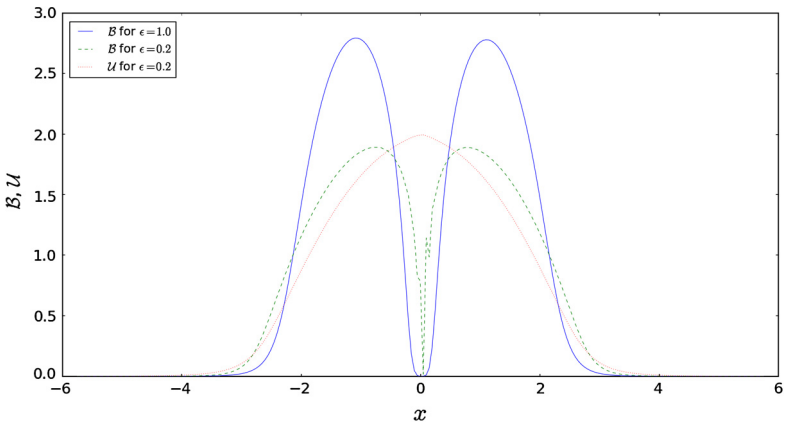

Fig. 3. Baryon density on a diagonal line through the centre of the $B = 4$ skyrmion for $\varepsilon = 1$ and $\varepsilon = 0.2$. The dotted red curve shows $\mathcal{U}(\varphi(x))$ for $\varepsilon = 0.2$, where $\mathcal{U}$ is the square root of the potential (see Eq. 2.4). (For interpretation of the references to color in this figure legend, the reader is referred to the web version of this article.)

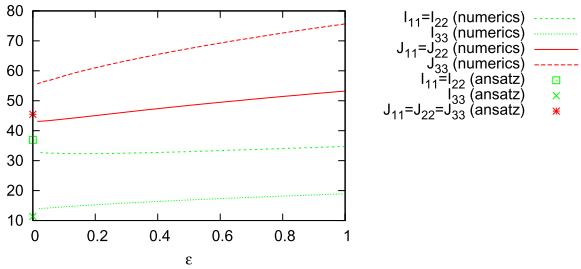

Fig. 4. Moments of inertia for the skyrmion with $B = 2$. The non-zero components of the leading terms in the ε-expansion given in (2.16) are plotted for a range of values of ε, together with the predictions from the ansatz $\varphi_H \circ \psi_2$.

$$J_{ij}(\varphi) = \int_{\mathbb{R}^3} \mathcal{B}(x)^2 (r^2 \delta_{ij} - x_i x_j) \mathrm{d}^3 x + O(\varepsilon), \tag{2.16}$$

respectively. For $\varphi_H \circ \psi_B$, J in particular is isotropic to leading order, $J = \mathrm{const}\, \mathbb{I}_3 + O(\varepsilon)$, a very strong constraint which is not supported by the numerical data: see Fig. 4.

Since all the minimisers are axially symmetric for $B = 1$ and $B = 2$, the E_ε minimisation problem can be reduced to two dimensions in these cases. We seek minimisers of the form

$$\varphi(\rho, z, \phi) = (n_1(\rho, z), n_2(\rho, z) \cos B\phi, n_2(\rho, z) \sin B\phi, n_3(\rho, z)) \tag{2.17}$$

where $(x_1, x_2, x_3) = (\rho \cos\phi, \rho \sin\phi, z)$, and $\boldsymbol{n}$ is a map from the right half-plane to S^2 which maps the z-axis onto the great circle $n_2 = 0$. The energy of such a map is

$$E_\varepsilon(\boldsymbol{n}) = 2\pi \int_{(0,\infty)\times\mathbb{R}} \Big\{ \varepsilon(|\partial_\rho \boldsymbol{n}|^2 + |\partial_z \boldsymbol{n}|^2 + \frac{B^2}{\rho^2} n_2^2) + \frac{B^2}{\rho^2} (\partial_\rho n_1 \partial_z n_3 - \partial_z n_1 \partial_\rho n_3)^2 + (1 - n_1)^2 \Big\} \rho \mathrm{d}\rho \mathrm{d}z. \tag{2.18}$$

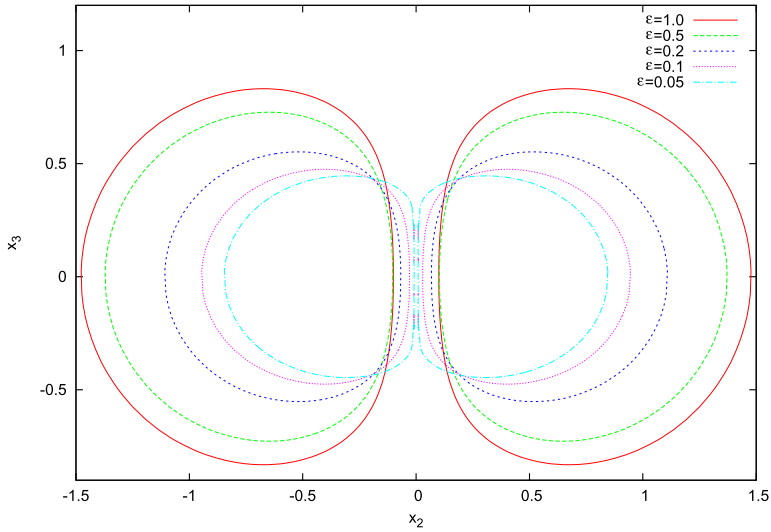

Fig. 5. Baryon density contours $\mathcal{B} = 1.8$ in the plane $x_1 = 0$ for the $B = 2$ skyrmion at various values of ε.

This integral was minimised using a (zero temperature) simulated annealing algorithm. A logarithmic lattice was used for ρ with lattice spacings $h = 0.05$ in $\ln \rho$ and z. The ranges of $\ln \rho$ and z were $[-5, 2]$ and $[0, 7.5]$, and partial derivatives were replaced by first order differences. In practice we found that minimising a discretisation of the difference between the energy and its topological lower bound, rather than of the energy, improved the performance of the algorithm.

As expected, the $B = 1$ minimiser is spherically symmetric, while the $B = 2$ minimiser has deformed toroidal level sets of $\mathcal{B}$. As $\varepsilon \to 0$, the hole through the centre of these tori closes up, and the level sets develop singularities along the symmetry axis, see Fig. 5. The reduction in dimension allows us to use a much finer grid, adapted to resolve the structures developing near the symmetry axis, so we can follow the solutions reliably down to much lower ε than is possible with the fully three-dimensional, method. The virial quantity $|D(\epsilon)|$ remained less than 1% for all minimisers that we found (D was not required to be positive in these simulations, as the use of a logarithmic grid for ρ effectively cuts out a neighbourhood of the x_3-axis). The difference in energies of the axial and 3D simulation results were $< 0.07\%$ for $B = 1$ and $< 0.18\%$ for $B = 2$.

Any static solution of the sextic model with $\varepsilon > 0$ must satisfy an interesting property called *restricted harmonicity* [13]. If φ is a critical point of E_ε, then $E_\varepsilon = E^{(6)} + E^{(0)} + \varepsilon E^{(2)}$ is critical with respect to all smooth variations of $\varphi : \mathbb{R}^3 \to S^3$, and hence, in particular, with respect to all variations of the form $\varphi_t = \varphi \circ \psi_t$, where ψ_t is a curve through the identity element in the group of volume preserving diffeomorphisms of $\mathbb{R}^3$. Now, as already observed, $E^{(0)}$ and $E^{(6)}$ are invariant under volume preserving diffeomorphisms, so it follows that $E^{(2)}$ itself must be critical with respect to such variations. This is precisely the condition for φ to be restricted harmonic, in the terminology introduced in [13], where it was shown that restricted harmonicity is equivalent to the condition that $\operatorname{div} \varphi^* h$ is an exact one-form. Here h denotes the Riemannian metric on the target space (in this case, S^3). Since $H^1(\mathbb{R}^3) = 0$, this is equivalent to the third order nonlinear PDE

$$\mathrm{d}(\operatorname{div} \varphi^* h) = \partial_k \partial_i (\partial_i \varphi \cdot \partial_j \varphi) dx_k \wedge dx_j = 0. \tag{2.19}$$

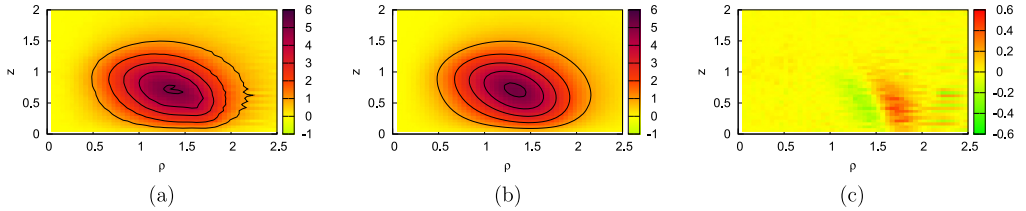

Fig. 6. Density plots for the left (a) and right (b) hand sides of the restricted harmonic equation (2.20) evaluated on the soliton with $\epsilon = 1$ and $B = 2$, and their difference (c). The plots show that Eq. (2.20) is satisfied to within numerical error.

For fields within the axially symmetric ansatz (2.17), this PDE reduces to

$$\rho^3(\partial_\rho \triangle \boldsymbol{n} \cdot \partial_z \boldsymbol{n} - \partial_z \triangle \boldsymbol{n} \cdot \partial_\rho \boldsymbol{n}) + \rho^2(\partial_\rho^2 \boldsymbol{n} \cdot \partial_z \boldsymbol{n} - \partial_\rho \boldsymbol{n} \cdot \partial_\rho \partial_z \boldsymbol{n})$$
$$= \rho \partial_\rho \boldsymbol{n} \cdot \partial_z \boldsymbol{n} - 2B^2 n_1 \partial_z n_1, \tag{2.20}$$

in which $\triangle = \partial_r^2 + \partial_z^2$. In Fig. 6 we present evidence that our axially symmetric $B = 2$ numerical solutions are approximately restricted harmonic. The restricted harmonic map equation is a closed condition on the space of all fields (with respect to any sensible choice of topology thereon). Since minimisers of E_ε for $\varepsilon > 0$ are restricted harmonic for all $\varepsilon > 0$, it follows that, if the minimisers converge to some limit as $\varepsilon \to 0$, this limit should likewise be restricted harmonic. This is another reason to be sceptical of the axially symmetric BPS skyrmions $\varphi_H \circ \psi_B$ used in [5,8–11]: it is known that, except for $B = 1$, none of these solutions are restricted harmonic [13], and that their failure to be so gets progressively worse as B increases.

Recall that the underlying motivation for this model is the hope that, for ε small and positive, it may support skyrmions with classical binding energies close to real nuclear physics data. So is $\varepsilon = 0.2$ small enough? Sadly, no. While $E_{0.2}$ supports skyrmions with significantly lower binding energies than those found in the conventional (massless or massive) Skyrme model, they are still much larger than those found in nature: see Fig. 11 in Section 4. We can use the results of our more refined axially symmetric simulations to predict roughly how small ε would need to be to give classical binding energies in the right ballpark. Real nuclei have binding energies per nucleon of around 1%, so we should demand that

$$\frac{BE_{min}(1,\varepsilon) - E_{min}(B,\varepsilon)}{BE_{min}(1,\varepsilon)} \approx 0.01. \tag{2.21}$$

Imposing this for $B = 2$ yields $\varepsilon = 0.014$, considerably beyond the reach of our main numerical scheme. (We use the rough figure 1% rather than fitting to the binding energy of the deuteron since the latter is anomalously small.) For ε so small, it is reasonable to hope that φ will be close to a BPS skyrmion, that is, a minimiser of $E_0 = E^{(6)} + E^{(0)}$. The question is, which one? Except for $B = 1, 2$ where enhanced symmetry allows a reduction in dimension, this question seems to be numerically intractable. Our results suggest that the minimisers converge as $\varepsilon \to 0$ to BPS skyrmions of low regularity, which typically have strings of conical singularities, and which preserve the property of restricted harmonicity.

3. The lightly bound model

The lightly bound model is defined by adding to Skyrme's lagrangian (1.1) a term proportional to $\mathrm{Tr}(1-U)^4$. After fixing units of energy and length, this model depends on two non-trivial parameters. In suitable units, the associated static energy functional takes the form

$$E = \int_{\mathbb{R}^3} \Big[(1-\alpha)\left(-\frac{1}{2}\mathrm{Tr}(R_i R_i) + m^2 \mathrm{Tr}(1-U) \right) - \frac{1}{16}\mathrm{Tr}([R_i, R_j][R_i, R_j]) + \alpha(\tfrac{1}{2}\mathrm{Tr}(1-U))^4 \Big] \mathrm{d}^3x. \tag{3.1}$$

Here $\alpha \in [0,1]$ and $m := (2m_\pi\sqrt{1-\alpha}/F_\pi g) \geq 0$ are dimensionless parameters. In writing the energy in this way, we have implicitly chosen $F_\pi/4g\sqrt{1-\alpha}$ as a unit of energy and $2\hbar c\sqrt{1-\alpha}/F_\pi g$ as a unit of length. The advantage of parameterising the model in this way is that soliton energies and sizes remain roughly constant as α is varied, thus enabling simulations with a range of values of α to be performed on the same grid. In the limiting case $\alpha = 1$ the above model has a topological energy bound $E \geq 8\pi^2|B|$ which can be saturated only in the $|B| = 1$ sector [6]. Solitons with $|B| > 1$ are therefore unstable to fission. The other extreme case $\alpha = 0$ is the standard massive Skyrme model, in which binding energies are too large.

Numerical approximations to minima of the lightly bound energy (3.1) with B between one and eight have been determined for a range of values of α and for $m = 1$. Fixing the value of m ensures that the Compton wavelength of the pion remains comparable to the size of a nucleus, as nuclear radii do not depend strongly on the value of α.

To simulate the model for a given α numerically we used the same numerical scheme as in Section 2 on a cubic lattice of size N^3 with $N = 301$ and lattice spacing $h = 0.05$. We obtained a lattice approximant to the energy for a given value of α, E_α for one or more (perhaps only local) energy minima in each charge sector. A wide range of initial conditions were used to assist in finding the global energy minimiser for each baryon number considered. The accuracy checks, already described, were applied. Firstly, the baryon number was calculated using the formula (1.2) and evaluated using the same scheme. The value obtained was correct to within 0.001% of the integer value. Secondly, the virial constraint $D(\alpha)$, similar to (2.14), was evaluated on energy minima (in which $E^{(a)}$ denotes the component of the energy involving a derivatives):

$$D(\alpha) := \frac{1}{E}(E^{(4)} - E^{(2)} - 3E^{(0)}) = 0. \tag{3.2}$$

When evaluated on our numerically-determined minima this quantity was at worst 0.01%.

For B between one and four the full range of α was explored. Two sets of simulations were performed: one in which the minima were initially determined for $\alpha = 0.95$ and tracked as α decreased to 0 in steps of 0.05, and one in which the minima were initially determined for $\alpha = 0$ and tracked as α increased to 0.95 in steps of 0.05. Both sets of simulations gave similar results for α close to 0 and 0.95. For small α the minima were qualitatively similar those of the Skyrme model and in particular shared their symmetry groups. For α near 0.95 energy densities of minima were localised at B points, which we interpret as the locations of the B nucleons within the nucleus. The transitions between the two types of soliton occurred at different values of α according to whether α was increasing or decreasing. For α increasing the transitions occurred when $\alpha \in [0.4, 0.5]$, while for α decreasing they occurred when $\alpha \in [0.35, 0.4]$.

Energy minima were examined more carefully for $\alpha \in [0.9, 1.0]$ and B between one and eight. This range of α is the one in which binding energies are comparable to experimental values. We

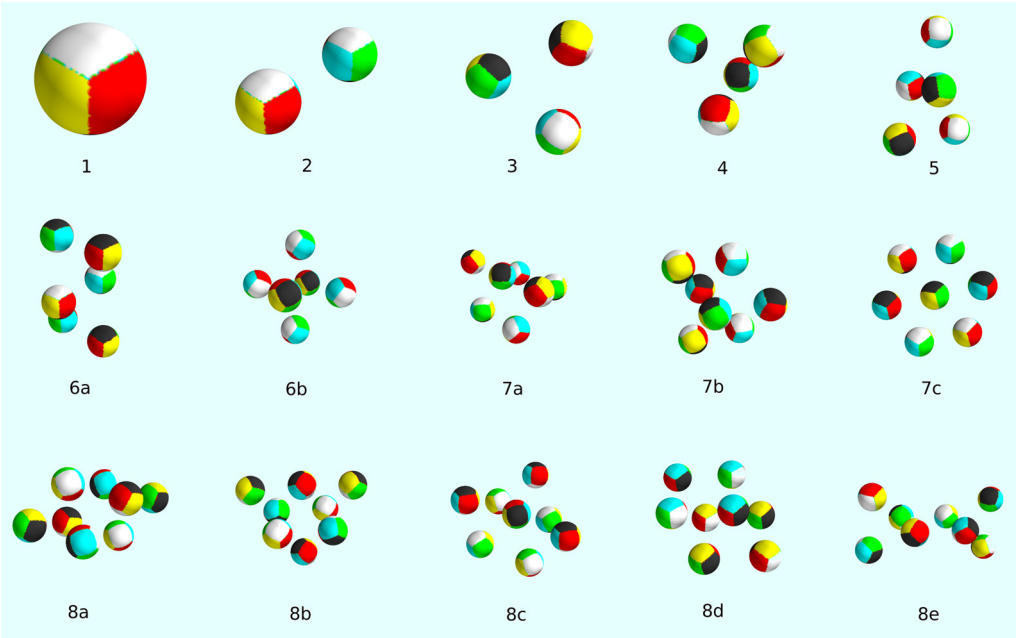

Fig. 7. Baryon density isosurfaces of skyrmions in the lightly bound model.

Table 1
Energies, isoscalar charge radii, and binding energies per nucleon of skyrmions in the lightly bound model with $\alpha = 0.95$.

Configuration	$E/8\pi^2$	$\sqrt{\langle r^2 \rangle_{I=0}}$	BEPN (MeV)	$\sqrt{\langle r^2 \rangle_{I=0}}$ (fm)
1	1.1082	1.2457	0.00	0.8104
2	2.2119	2.2261	1.84	1.4481
3	3.3129	2.7627	3.26	1.7971
4	4.4111	2.9310	4.56	1.9066
5	5.5132	3.4593	4.66	2.2503
6a	6.6128	3.4426	5.09	2.4190
6b	6.6130	3.4426	5.07	2.2394
7a	7.7120	3.5350	5.45	2.2995
7b	7.7127	3.8888	5.36	2.5297
7c	7.7140	4.1668	5.21	2.7105
8a	8.8090	4.0367	5.95	2.6259
8b	8.8094	3.9610	5.91	2.5766
8c	8.8124	4.1150	5.59	2.6768
8d	8.8130	4.1431	5.52	2.6951
8e	8.8130	4.1430	5.52	2.6950

found that $\alpha = 0.95$ gave binding energies of appropriate magnitude relative to the proton mass; baryon density isosurfaces for the minima that we found are displayed in Fig. 7. Note that for $B \geq 6$ several local minima of the energy have been found. The isosurfaces have been coloured to indicate the orientation of the pion fields on the surface, as described in the previous section. The energies of these configurations are recorded in Table 1. Also recorded in this table are their charge radii $\sqrt{\langle r^2 \rangle_{I=0}}$, defined by the formulae

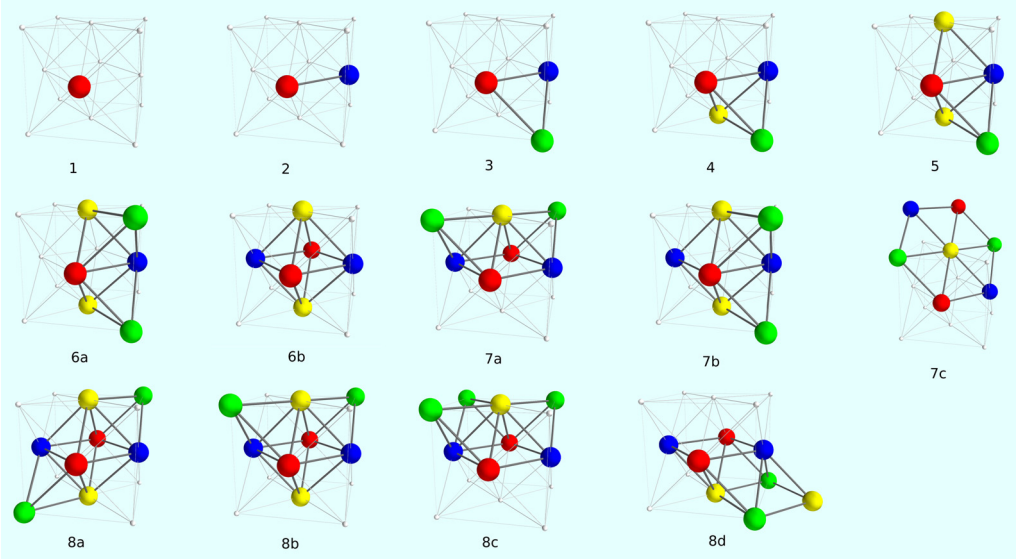

Fig. 8. Subsets of the face-centred-cubic lattice corresponding to the isosurfaces in Fig. 7.

$$\langle r^2 \rangle_{I=0} = \frac{1}{2\pi^2 B} \int_{\mathbb{R}^3} \|\mathbf{x} - \mathbf{x}_0\|^2 \, \mathcal{B}(\mathbf{x}) \, \mathrm{d}^3 x, \quad \mathbf{x_0} = \frac{1}{2\pi^2 B} \int_{\mathbb{R}^3} \mathbf{x} \, \mathcal{B}(\mathbf{x}) \, \mathrm{d}^3 x. \tag{3.3}$$

The most striking feature of the baryon density isosurfaces is that they display a clear particle-like structure. This is in marked contrast with the traditional Skyrme model, in which individual nucleons are not discernible within a nucleus. The value of $0.1 \max\{\mathcal{B}\}$ used to create the isosurfaces in Fig. 7 is significantly lower than those commonly used in the Skyrme model; if instead a larger value of $\mathcal{B}$ is used the particle-like structure is even more pronounced. The points at which $\mathcal{B}$ attains local maxima are close to the B points at which the field U takes the value -1. Unlike in the usual Skyrme model these preimage points are non-degenerate. The likely cause of this is the choice of potential in our model, which strongly disfavours U being close to -1. The standard potential $\mathrm{Tr}(1 - U)$ has a similar but weaker effect: with this potential -1 has two preimage points with four-fold degeneracy in the $B = 8$ soliton, whereas without it -1 has a single preimage point with eight-fold degeneracy.

Another remarkable feature evident in Fig. 7 is that, with one exception, all configurations resemble subsets of a face-centred cubic lattice. Within each of these lattice-like configurations, no more than four distinct orientations for the constituent particles can be observed (corresponding to whether the particle is on a vertex of a cube, a horizontal face, or either of the two orientations for vertical faces). The precise subsets of the lattice are displayed in Fig. 8, with the four orientations distinguished by four colours. The only soliton to which these comments do not apply is configuration 8e. This configuration resembles a pair of adjacent tetrahedra and cannot be realised as a subset of the face-centred cubic lattice; its eight constituent particles all have different orientations.

In order to make a direct comparison between the lightly bound model and experimental nuclear physics we have calibrated our units of energy and length. The energy units were chosen so that the one-soliton had energy equal to the proton mass, 938.27 MeV. The length units were

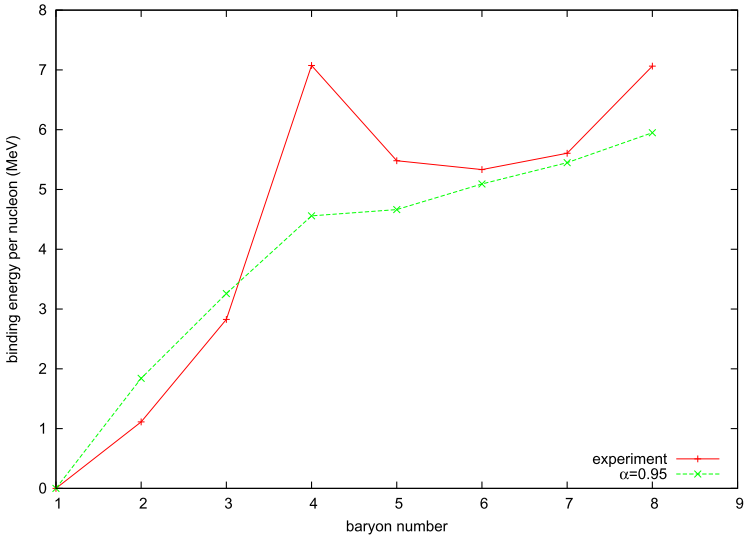

Fig. 9. Binding energy per nucleon as a function of baryon number in the lightly bound model and from experimental nuclear physics.

chosen by fitting the electric charge radii of the proton and neutron. If the proton and neutron are modelled as rigidly isospinning bodies centred at the origin then their charge radii are given by

$$\langle r^2\rangle_p = \int_{\mathbb{R}^3} r^2 \left(\tfrac{1}{4\pi^2}\mathcal{B} + \mathcal{I}_3\right) \mathrm{d}^3x, \quad \langle r^2\rangle_n = \int_{\mathbb{R}^3} r^2 \left(\tfrac{1}{4\pi^2}\mathcal{B} - \mathcal{I}_3\right) \mathrm{d}^3x, \tag{3.4}$$

where $\mathcal{I}_3$ denotes the isospin charge density, normalised such that $\int_{\mathbb{R}^3} \mathcal{I}_3 \mathrm{d}^3x = \frac{1}{2}$. We therefore identify

$$\sqrt{\langle r^2\rangle_{I=0}} = \sqrt{\langle r^2\rangle_p + \langle r^2\rangle_n} = \sqrt{0.8783^2 - 0.1149}\ \mathrm{fm} = 0.8103\ \mathrm{fm}. \tag{3.5}$$

These normalisation conventions force us to identify

$$\frac{F_\pi}{4g\sqrt{1-\alpha}} = 10.72\ \mathrm{MeV}, \quad \frac{2\hbar c\sqrt{1-\alpha}}{F_\pi g} = 0.6505\ \mathrm{fm}. \tag{3.6}$$

Hence the following values are chosen for the parameters in the Skyrme lagrangian (1.1):

$$F_\pi = 29.1\ \mathrm{MeV}, \quad m_\pi = 303\ \mathrm{MeV}, \quad g = 3.76. \tag{3.7}$$

With these units the pion decay constant is significantly below its experimental value of 186 MeV, and the pion mass is significantly above its experimental value of 138 MeV. Most calibrations of the standard Skyrme model result in abnormally low values of the pion decay constant. Although this problem seems to be exacerbated in the lightly bound model, we expect for reasons to be explained below that the value of F_π would increase in a quantised treatment of the model. A better value for the pion mass could be obtained by reducing the value of the parameter m in the model, but we have not explored this possibility. Reducing the value of m would probably reduce soliton energies, and thereby also increase the value of F_π.

The binding energy per nucleon is plotted alongside experimental values in Fig. 9. The theoretical binding energy per nucleon is calculated from the formula $E_B/B - E_1$, in which E_B

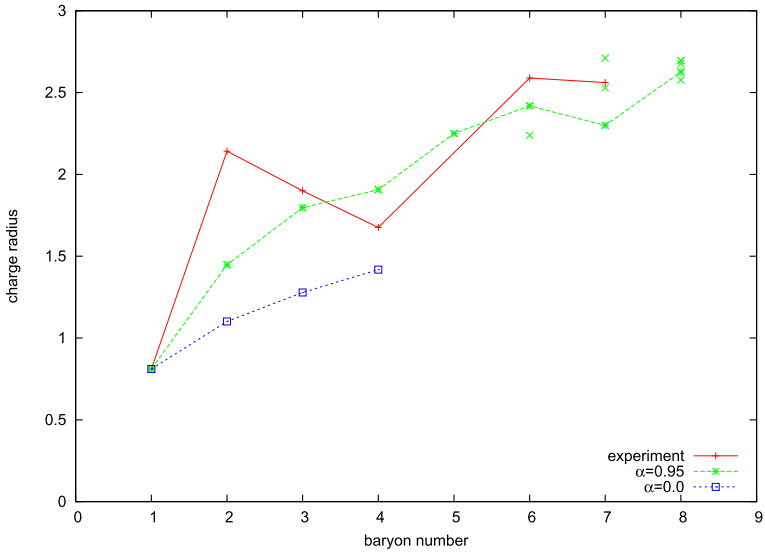

Fig. 10. Isoscalar charge radii in the lightly bound model ($\alpha = 0.95$), the standard Skyrme model ($\alpha = 0$), and from experimental nuclear physics. The $\alpha = 0.95$ curve passes through the points corresponding to global energy minima.

represents the global minimum of the energy in the charge B sector. The corresponding experimental values are the binding energies for the lightest isotope at each mass number B. The theoretical curve closely follows the experimental curve for most values of B in the range considered, except that the anomalies at $B = 4$ and 8 are less pronounced in the theoretical curve than in the experimental curve. This graph represents a substantial improvement on the standard Skyrme model (see Fig. 11 for a comparison).

The skyrmion isoscalar charge radii are plotted alongside experimental values in Fig. 10. For B even the experimental values shown are the charge radii of isotopes with mass number B and isospin 0. For B odd they are calculated as weighted averages of the states with isospin $I = \pm 1/2$ via the formula $\langle r^2 \rangle_{I=0} = [(B+1)\langle r^2 \rangle_{I=1/2} + (B-1)\langle r^2 \rangle_{I=-1/2}]/2B$. Like Eq. (3.5), this formula is motivated by identifying the $I = \pm 1/2$ states with solitons isorotating rigidly in opposite directions.

Fig. 10 shows that the theoretical and experimental charge radii are comparable. The most surprising feature of the experimental curve is the abnormally large radius at $B = 2$ in comparison to $B = 1$. The lightly bound model does not fully capture this feature, but approximates it better than the standard Skyrme model, which is plotted alongside for comparison.

4. Concluding remarks

We have investigated the problem of obtaining low binding energies in two variants of the Skyrme model. Our results are summarised in Fig. 11, alongside results obtained from a third "holographic" variant explored in [4], the standard Skyrme model, and the experimental binding energy curve. The sextic and holographic models are both capable, in principle, of producing skyrmions with very low binding energies, but in practice they are yet to yield realistic binding energies in numerical simulations. For the sextic model, the problem is that the skyrmions start to develop singularities, and become numerically inaccessible, before the regime of very low

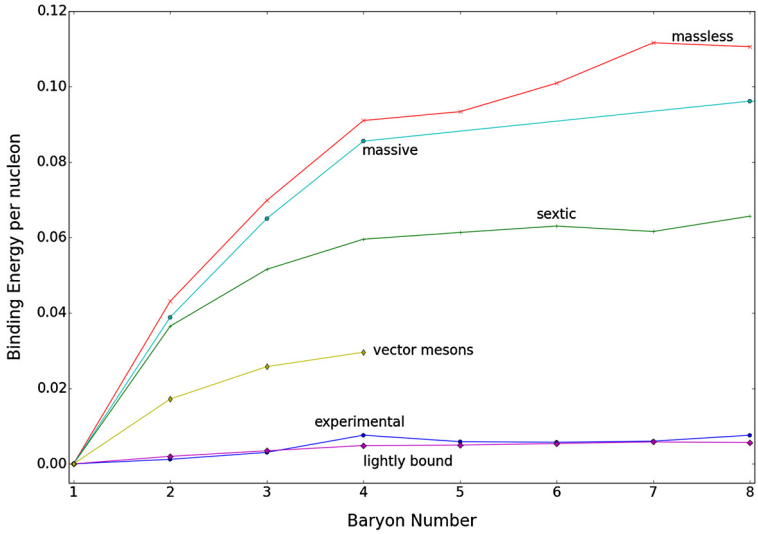

Fig. 11. Binding energy per nucleon for $B = 2, \ldots, 8$ in various variants of the Skyrme model: the *massless* Skyrme model with $m = 0$, the *massive* Skyrme model with $m = 1$, the *sextic* Skyrme model with $\varepsilon = 0.2$, holographic Skyrme model with *vector mesons*, the *lightly bound* Skyrme model with $\alpha = 0.95$ and *experimental* data. Markers indicate values of available data.

binding energy is reached. For the holographic model, which is a Skyrme model coupled to an infinite tower of vector mesons, only the lowest truncation level, including just the lightest vector meson and the lightest axial vector meson, has been treated numerically. One could, in principle, include more mesons from the tower, and this would presumably reduce the binding energies further. However the resulting model would be formidably complicated, and hence difficult to solve numerically in practice. In contrast, the lightly bound model looks very promising: using standard numerical algorithms, binding energies have been obtained which are comparable with experimental values. This model clearly deserves further attention.

The solitons obtained in the lightly bound model differ markedly from those obtained in the standard Skyrme model, in that they resemble a lattice of nucleons. This result suggests that the problem of finding solitons with higher baryon number could be simplified by first investigating a point particle model, along the lines of [7].

Our analysis of the lightly bound model has been purely classical, but in the future this model should be quantised semi-classically. Including quantum corrections would no doubt modify some of our results. Most notably, the masses of quantised states would be higher than the classical values quoted here, with the one-soliton affected more severely than others. Therefore binding energies are likely to be reduced in a semi-classical treatment, and the value chosen for α would need to be reduced to compensate for this. Reducing the value of α would also lead to a more realistic value for the pion decay constant.

Our attempts to obtain realistic binding energies within the sextic model have been hampered by numerical difficulties associated with the formation of singularities in the field. Thus a different numerical scheme is called for if any progress is to be made with this model. Despite these difficulties, we have found clear evidence that solitons in this model do not resemble the ansatz proposed in [5,8–11]. In this light it would be worthwhile therefore to revisit some of the results obtained therein.

Acknowledgements

This work was supported by EPSRC through the grant "Geometry, Holography and Skyrmions," EP/K003453/1. We acknowledge valuable conversations with Christoph Adam, Andrzej Wereszczynski, Paul Sutcliffe, and Nick Manton. The majority of simulations were performed using computer code originally developed in collaboration with Juha Jäykkä and utilised the ARC High Performance Computing facilities at the University of Leeds.

Appendix A. Energies in the sextic model

Table 2
Numerical values of energy and baryon number for skyrmions in Fig. 2. E_ϵ is given by (2.3).

Configuration	$\epsilon = 1$		$\epsilon = 0.2$	
	E_1	B	$E_{0.2}$	B
1	62.7543	0.999991	29.4172	0.999995
2	116.696	1.999981	56.6878	1.999972
3	169.146	2.999970	83.6968	2.999764
4	220.424	3.999964	110.659	3.999790
5	274.815	4.999958	138.065	4.999874
6	327.445	5.999950	165.374	5.999737
7	379.956	6.999939	193.238	6.999792
8a	433.719	7.999931	220.633	7.999514
8b	435.214	7.999934	219.884	7.999600

References

[1] E. Witten, Nucl. Phys. B 223 (1983) 433.
[2] R.A. Battye, et al., Phys. Rev. C 80 (2009) 034323, arXiv:0905.0099.
[3] R. Battye, N.S. Manton, P. Sutcliffe, Proc. R. Soc. Lond. A 463 (2007) 261, arXiv:hep-th/0605284.
[4] P. Sutcliffe, J. High Energy Phys. 4 (2011) 45, arXiv:1101.2402.
[5] C. Adam, J. Sánchez-Guillén, A. Wereszczyński, Phys. Lett. B 691 (2010) 105, arXiv:1001.4544.
[6] D. Harland, Phys. Lett. B 728 (2014) 518, arXiv:1311.2403.
[7] P. Salmi, P. Sutcliffe, J. Phys. A 48 (2015) 035401, arXiv:1409.8176.
[8] C. Adam, J. Sánchez-Guillén, A. Wereszczyński, Phys. Rev. D 82 (2010) 085015, arXiv:1007.1567.
[9] C. Adam, et al., arXiv:1306.6337, 2013.
[10] E. Bonenfant, L. Marleau, Phys. Rev. D 82 (2010) 054023, arXiv:1007.1396.
[11] E. Bonenfant, L. Harbour, L. Marleau, Phys. Rev. D 85 (2012) 114045, arXiv:1205.1414.
[12] K. Arthur, et al., J. Math. Phys. 37 (1996) 2569.
[13] J.M. Speight, arXiv:1406.0739, 2014.
[14] J. Jäykkä, J.M. Speight, Phys. Rev. D 84 (2011) 125035, arXiv:1106.5679.
[15] G.H. Derrick, J. Math. Phys. 5 (1964) 1252.
[16] I. Floratos, B. Piette, Phys. Rev. D 64 (2001) 045009.